Impact of Tire Loading and Tire Pressure on Measured 3D Contact Stresses

Jaime A. Hernandez[1], Imad Al-Qadi[2], and Morris De Beer[3]

[1]PhD Candidate, Illinois Center for Transportation, Department of Civil and Environmental Engineering, University of Illinois at Urbana-Champaign, email: hrnndzr2@illinois.edu
[2]Founder Professor of Engineering, Illinois Center for Transportation, Director, University of Illinois at Urbana-Champaign, email: alqadi@illinois.edu
[3]Principal Researcher, Transport Infrastructure Engineering, Council for Scientific and Industrial Research, email: mbeer@csir.co.za

ABSTRACT

Three-dimensional (3D) tire–pavement contact stresses for two types of tires used by the truck industry (new generation wide-base tire [WBT] and dual-tire assembly [DTA]) were measured and compared. The testing matrix was composed of five loads (P) (26.6, 35.5, 44.4, 62.1, and 79.9 kN) and four tire inflation pressures (σ_o) (552, 690, 758, and 862 kPa). The equipment used for measuring the 3D- contact stresses is described along with the testing procedure and the methodology followed during data processing. The effect of applied load and tire-inflation pressure on the variation of longitudinal, transverse, and vertical CONTACT STRESSES along the contact length of each tire type was analyzed. Differences in the distribution and magnitude of the aforementioned stresses were observed between WBT and DTA; these differences are an important factor linked to pavement damage caused by each tire configuration. This experimental effort is part of a national study to evaluate the effect of WBT on pavement damage and compare it to that of DTA.

INTRODUCTION

Successful analysis and design of pavements is strongly related to appropriate consideration of environmental factors (e.g., temperature and moisture), material characterization, and traffic. Traffic is defined by a series of factors, including tire structure, load magnitude, and inflation pressure. These three elements are intrinsically related to each other. The mechanistic-empirical pavement design guide (ME-PDG) (ARA 2004) unifies the relationship of these factors by assuming the contact between tire and pavement is circular and stresses at the tire–pavement interface are uniform in only the vertical direction. Experimental evidence demonstrates that these assumptions are invalid and shows that three-dimensional (3D) nonuniform contact stresses are a more accurate representation of tire–pavement interaction (De Beer et al. 1997, Al-Qadi and Yoo 2007).

Efforts to measure contact stresses are not recent. As early as 1959, the Council for Scientific and Industrial Research (CSIR) in South Africa (Bonse and Kuh 1959) developed a measuring device composed of a stress recorder box and mobile electronic and photographic equipment for roadside use. The equipment measured forces in the three principal directions. The measurements showed that vertical stresses were affected mainly by tire inflation pressure and longitudinal stresses by tire torque.

In the 1970s and 1980s, three apparatus were proposed. The first, developed at Technische Universität München, pressed a rotating tire against a rotating drum

composed of a measuring mechanism (Seitz and Hussmann 1971). With the second, a steel road bed (12.2 m long and 0.41 m wide), macroforce transducer (0.27 m wide and 0.25 m long), and minitransducer (5.1 mm diameter for circle or 5.1 mm per side for square) were used to read forces and moments in the three principal directions (Lippmann and Oblizajek 1974). Finally, a set of ten beams instrumented with strain gauges distributed along the cross length of a tire was implemented by Howell et al. (1986) and applied to aircraft tires.

A servo-hydraulic system where the tire position is fixed and the loading plate is moved against the tire was introduced in Texas (Tielking 1994). The dimensions of the loading plate were 505 × 505 × 76.2 mm, and it contained 10 pins in the cross-direction of the tire. Each pin was instrumented with three strain gauges. The pins were separated 25 mm (center to center) so that more than one reading could be captured in each rib. The effect of tread wear, offset wheel flange, and footprint location on footprint was reported. Himeno et al. (1997) linked pavement distresses to tire–pavement contact stresses. The equipment used in that study consisted of 64 sensors separated 15 mm; each pin had a section of 14 × 18 mm. Only vertical measurements were reported. It was concluded that vertical stresses greatly depended on the tire type and the tread pattern and that average vertical pressure was not influenced by the tire inflation pressure or speed. More important, the relevance of different assumptions regarding contact stresses on the calculation of the pavement life was highlighted. The Stress-In-Motion (SIM) system was developed by De Beer et al. (De Beer et al. 1997). With that system, De Beer et al. demonstrated the contrast between the response of thin flexible pavements using uniform and nonuniform 3D contact stresses and established the importance of appropriate consideration of tire–pavement interaction.

Myers et al. (1999) explained the influence of tire structure on contact stresses distribution and pointed out the relevance of transverse tractions on the development of surface distresses (surface cracking and near-surface rutting). The conclusions were based on measurements made with an apparatus composed of 16 coaxial load and displacement transducers in the tire's transverse direction. A different approach was used by Anghelache et al. (2003): a free rolling car tire was loaded against a table that moved in the longitudinal direction. The longitudinal and transverse tractions were measured using eight beam-type transducers. Every beam-type element had strain gauges. These elements were placed inside the movable table, and the upper face coincided with the movable table's surface. According to the authors, increment in applied load and decrement in tire inflation pressure caused important growth in contact length and maximum longitudinal contact stresses.

The most recent measuring device was reported in the literature in 2011 (Anghelache et al. 2011). The device is composed of 30 L-shaped steel sensing elements with, 10 × 10 mm square contact area (resistive strain gauges). The device measures contact stresses under different rolling conditions, but it is applicable only to car tires.

Even though significant efforts have been made to fully understand tire–pavement interaction, not many studies have focused on truck tires and their effect on pavement response. In the current project, the authors studied contact stresses of the most common type of tire used by the truck industry (dual tire assembly [DTA]) and an

emerging alternative (new generation wide-base tire [WBT]). The effect of applied load and tire inflation pressure on contact stresses distribution and magnitude is discussed in this paper. The experimental device used for the measurements, data processing, and information extracted from the experimental measurements are presented. Stresses in each direction and the effect of selected variables are analyzed. Finally, the contact area and contact length of various tire loading combinations are presented and discussed.

EXPERIMENTAL PROGRAM

Three-dimensional (3D) tire–pavement contact stresses were measured for two types of tires: new generation wide-base tires (445/50R22.5) and dual tire assembly (275/80R22.5), referred to in this paper as WBT and DTA, respectively. Four values of tire inflation pressure (σ_o) at 512.0, 690.0, 758.0, and 862.0 kPa, and five tire loadings (P) at 26.6, 35.6, 44.4, 62.1, and 79.9 kN, were applied to the tires to measure the 3D contact stresses.

The dual SIM Mk IV system used in this study for the measurements consisted of two SIM pad assemblies, each 840 × 471 mm in nominal area. A single SIM pad assembly of the SIM Mk IV tire contact load/stress measurement system consisted of an array of 21 instrumented steel pins laterally across the center portion of the SIM pad assembly. In addition to the instrumented pin assemblies, supporting pins on both sides of the instrumented pins (approximately 1020 for each SIM pad) supported the test tire during SIM testing. These conical-shaped pins of approximately 50 mm in height were fixed to a 45-mm-thick rigid steel base plate. The friction characteristics of the surface of these SIM test pads approximated those of an average dry asphalt concrete surface (De Beer et al. 1997).

In the current study, the test tires were fixed to the axle on the hydraulic loading test carriage of the Heavy Vehicle Simulator (HVS Mk III). The test tires were also fixed in the lateral position over the dual SIM pads for all measurements in this test series. The WBT tire was also fixed over the center portion of the dual SIM pads for all its measurements. Therefore, no lateral shifts were allowed during SIM testing. The vertical contact stresses were assumed positive in the vertical downward direction, while positive longitudinal tractions pointed in the traffic direction. The direction of positive transverse tractions can be inferred from the right-hand rule. The average tire speed was 0.331 m/s and the sampling frequency was 1001 Hz.

Static tire ink imprints were made using black roof paint on white paper (160 gm/m^2) under the HVS Mk III. The aim was to obtain prints for the target loads indicated in the test matrix. After the tire ink imprints were made at the HVS test site, photos were taken of each case (per the test matrix) and then scaled in Excel spreadsheets. To calculate the contact area reported here, the tire footprints were imported and properly scaled in AutoCAD.

DATA PROCCESING

The SIM measurements were reported in .txt format. Each file reported the readings of the 42 instrumented pins in one of the three directions and its own measuring test speed and applied SIM total load (in kN). As stated before, the SIM load distribution measurements were reported in load units (N). For contact stresses these data values were converted to "effective contact stress" values in kPa by applying the "effective area" geometrical conversion factor of 0.25028 mm^2 to the

load data. Details of this SIM geometrical factor were explained by De Beer et al. (1997).

The experimental stress readings were filtered using the moving average method with a window size of 20 measurements. The same value was used for all data files, and it was selected based on the final smoothness and small shift of the data. The distance along the tire contact patch was obtained using the sampling frequency and the speed of the tire in each measuring case.

Generally speaking, the shape of distribution of the vertical and transverse contact stresses (σ_z and σ_y, respectively) was very similar, even though their magnitudes were different. σ_z and σ_y were zero at the beginning and end of the contact length and had a maximum value around the center of the tire. The location of this maximum value varied with the tire's acceleration (Bonse and Kuh 1959). The location of the maximum was consistently close to the center. In some cases, σ_y showed a negative at the end of the contact length, whose magnitude was small when compared to the positive peak.

On the other hand, the variation of the longitudinal contact stresses (σ_x) varied according to the rib's location. When the rib was at the edge of the tire, the distribution had three peaks: two negative and one positive. The first negative peak was located at the tire's front part, and its magnitude was comparable to the positive one. The second negative peak was greater than the other two extreme values, and it was located at the end of the contact length. If the rib was not an edge one, the negative peak at the tire's end vanished, and its distribution had only two peaks (one positive and one negative). In this case, the magnitude of the positive peak (rear part of the tire) was significantly higher than that of the negative peak. The value and location of the described peaks for each entry of the test matrix were extracted from every measuring pin.

The contact length used in the analysis was determined based on σ_z, and it was defined as the distance at which σ_z is not zero in each measurement. For each loading case, the maximum value of contact length was selected

VERTICAL CONTACT STRESSES

The variation of the maximum vertical contact stresses $\sigma_{z,max}$ with P and σ_o for each rib and tire type is presented in Figure 1. Since more than one measuring pin was in contact with any given rib, the value reported in this figure is the *maximum* among the pins under each rib. The plots are arranged in a matrix fashion where each column represents a testing scenario (WBT and DTA) at the same value of P.

Previously reported "n" and "m" shape patterns were seen as P increased from 26.6 to 79.9 kN at the same σ_o. The n- shape was clearer for DTA at low P than for WBT; the difference between $\sigma_{z,max}$ of a central rib and an edge rib was greater for DTA than for WBT. This indicates that WBT distributed the applied load more uniformly across the tire under intermediate and low P. However, for an edge rib, σ_z was significantly higher for WBT than for DTA if high load was applied. It should be noted that minima and maxima of the measured contact stresses depend also on the tire tread pattern, and that the position of lateral grooves may therefore influence the results. However, the selection of reporting on the maxima only, is therefore considered conservative.

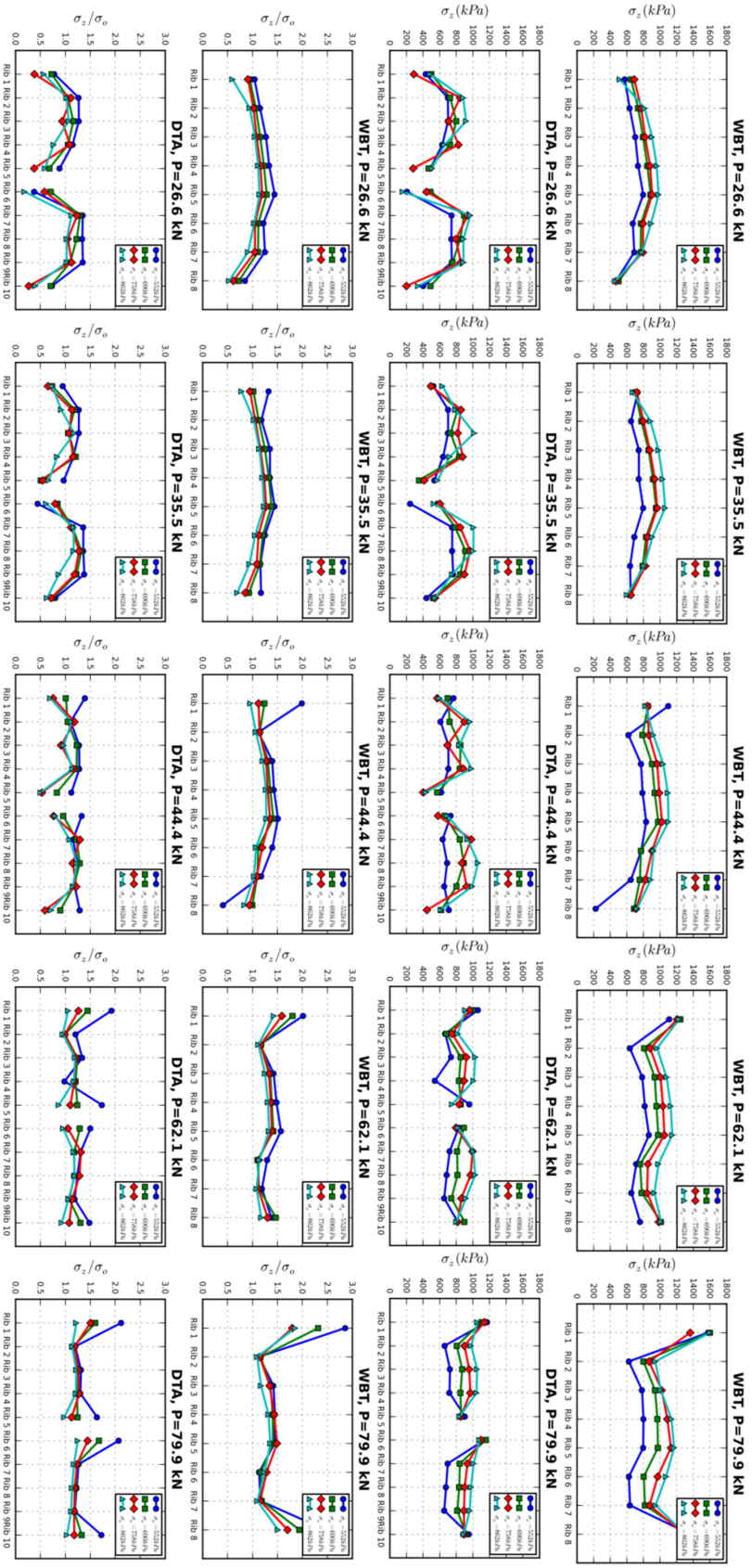

Figure 1. Maximum σ_z in each rib, and Maximum σ_z in each rib *normalized* with respect to σ_o for WBT and DTA

Figure 1 also shows the vertical stresses but *normalized* with respect to the corresponding σ_o. Even though, as expected, the shape of the plots did not change, the effect of σ_o on the *normalized* σ_z ($\bar{\sigma}_z = \sigma_z/\sigma_o$) was different than on σ_z only: $\bar{\sigma}_z$ decreased as σ_o increased. It was also observed that the range of values for which $\bar{\sigma}_z$ varied for a constant value of P was not wide, and it decreased as P is increased. Almost no values of $\bar{\sigma}_z$ in the central ribs were less than 1 in any case; this proves, once more, that assuming vertical contact stresses equal to σ_o was inaccurate. Moreover, $\bar{\sigma}_z$ can be as high as 2.8 (σ_z = 2.8 σ_o), as for WBT when P = 79.9 kN and σ_o = 552.0 kPa.

Figure 2 shows the variation of the maximum σ_z of each entry in the test matrix with σ_o and P. For both types of tires, the described maximum σ_z increased linearly with σ_o for a fixed value of P, as long as P was low ($P \leq 35.5$ kN for WBT and $P \leq 44.4$ kN for DTA). In the case of DTA, when $P > 44.4$ kN, σ_o did not have a relevant influence on the maximum σ_z, as indicated by the small slope of the corresponding lines. The relationship between the maxima with respect to each of the two tire types is also shown in Figure 2. The equality line is also presented in the same comparative plot. Most of the points lay on the right-hand side of the equality line. The points were located farther from the equality line as P increased. This implies two things: first, the maximum σ_z was almost always greater for WBT than for DTA; second, the difference in magnitude increased as P increased. Notice that for relatively low values of P, the associated data points were relatively close to the equality line.

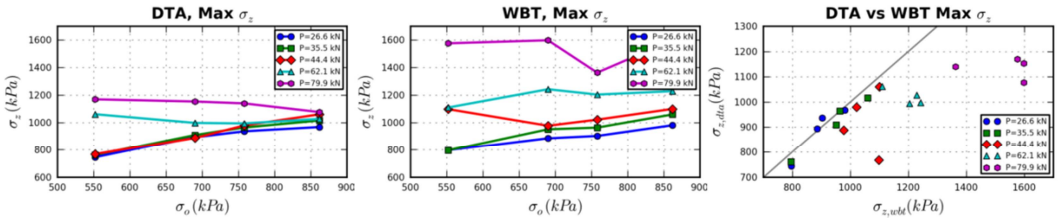

Figure 2. Variation of maximum σ_z with σ_o, and relationship between maximum σ_z of WBT and DTA.

TRANSVERSE AND LONGITUDINAL CONTACT STRESSES

The relationship between the *normalized* transverse contact stresses $\bar{\sigma}_y$ and $\bar{\sigma}_x$ for the considered types of tire, σ_o, and P is presented in Figure 3. It is known that σ_y is maximum at the edges of the rib and is negligible at its center. The values of $\bar{\sigma}_y$ in the plots are magnitudes (absolute value) of the maximum σ_y *normalized* with respect to σ_o at the edges of the ribs, i.e. σ_y/σ_o.

For WBT, the ratio between $\bar{\sigma}_y$ and $\bar{\sigma}_z$ for most points varied between 20% and 40% when the tire was subjected to relatively low values of P (26.6 and 35.5 kN), regardless of σ_o. As the load increased, the points were scattered between 10% and 40%. Values above the 40% and below the 10% line were fairly rare. The maximum value of the transverse contact stress was $\sigma_y = 0.5\sigma_o$ and corresponded to σ_o = 552.0 kPa and P = 62.1 kN.

For DTA, the variation was slightly different. First, the 20% line was no longer a lower boundary, and data varied between 0% and 40%. However, that was not the case if P = 79.9 kN, where most of the values lay between 0.2 $\bar{\sigma}_z$ and 0.5 $\bar{\sigma}_z$. For DTA, the maximum σ_y was given by the same loading condition as for WBT (σ_o = 552.0 kPa and P = 62.1 kN), and its value was 0.392 σ_o.

It is clear that the magnitude of the transverse contact stresses is relevant when compared to σ_z. This has important consequences in the analysis and design of flexible pavements. The relationship between transverse tractions and shear flow (plastic deformation) has been reported in the literature (Al-Qadi and Yoo 2007).

Figure 3 also compares the normalized longitudinal contact stresses $\bar{\sigma}_x$ with $\bar{\sigma}_z$. The plots are arranged as vertical and transverse cases: each row corresponds to the same tire type, and each column represents the same value of P. As described above, depending on the location of the rib, the distribution of σ_x contained 2 or 3 extreme values. For the sake of comparison, the ribs at the edge of the tire were omitted in these plots since the distribution was different and often the maximum σ_x was associated with a negative peak. Most of the $\bar{\sigma}_x$ data were lower than 0.2 σ_z in the case of WBT; however, some values were close to 0.4 σ_z. The upper boundary shifted from 40% to 35% of σ_z for DTA.

CONTACT AREA AND CONTACT LENGTH

The variation of the contact area Ac with σ_o for each value of applied load and type of tire is presented in Figure 4. The variation of Ac tended to be linear for both types of tires, even though the degree of the variation (slope of each line) was slightly higher for DTA than for WBT. As expected, Ac decreased as P decreased and σ_o increased. Figure 4 compares the contact area for both the WBT and DTA. The Ac for DTA was greater compared with WBT; the range of variation was between equality at P = 79.9 kN and σ_o = 862.0 kPa and approximately 38% greater at P = 26.6 kN and σ_o = 552.0 kPa.

Finally, a similar set of plots, dealing with maximum contact length l, are given in Figure 5. Figure 5 illustrates the variation in contact length for DTA and WBT with σ_o and P and depicts a comparison of the maximum contact length of each type of tire. The maximum contact length of both types of tires decreased as tire inflation pressure increased, and it increased as the load increased. These variations were linear for all the analyzed cases. This fact is verified in Figure 5, which depicts a linear fit with a high coefficient of correlation. The linear regression shows that the maximum contact length for DTA l_{dta} was approximately 65% smaller than the maximum contact length for WBT l_{wbt}.

Different mechanism in the load distributions in each tire were observed. While DTA had a higher contact area than WBT, the maximum contact length for WBT was longer than for DTA. It is important to recall that maximum σ_z was consistently higher for WBT. In other words, to distribute the same load at the same tire inflation pressure, DTA required greater contact area and shorter maximum contact length, and it generated smaller maximum vertical contact stresses than WBT did.

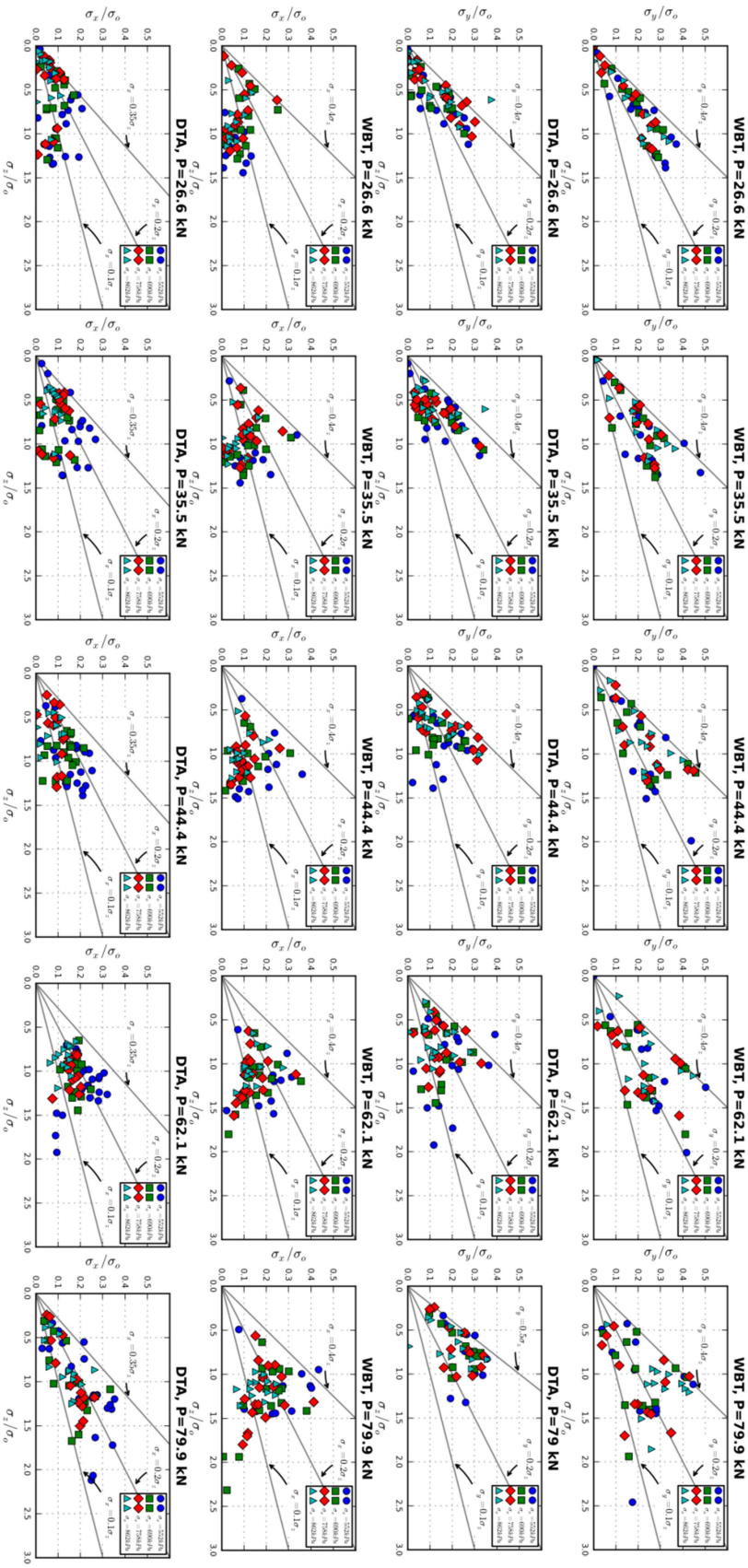

Figure 3. Relationship between maximum σ_z/σ_o and σ_y/σ_o and between maximum σ_z/σ_o and σ_x/σ_o

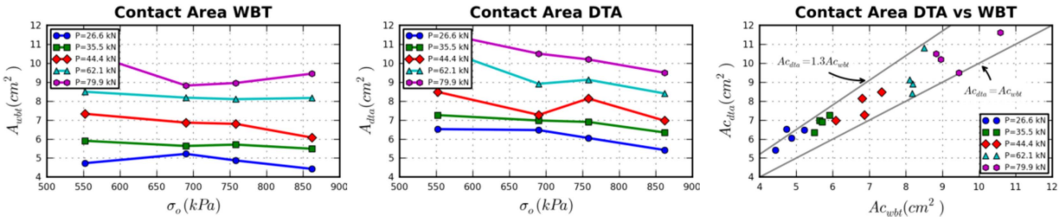

Figure 4. Variation of contact area for WBT and DTA, and relationship between contact area for WBT and DTA.

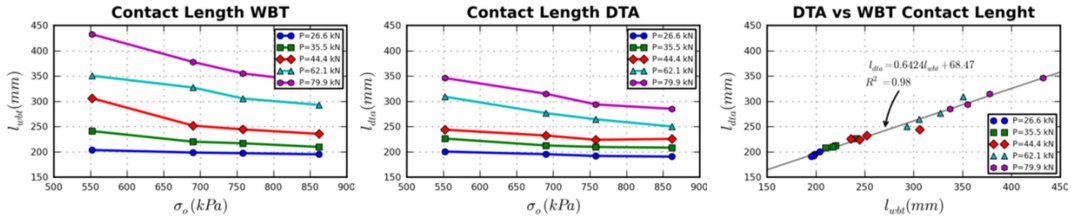

Figure 5. Variation of contact length for WBT and DTA, and relationship between contact length for WBT and DTA.

SUMMARY

Comparisons between three-dimensional tire–pavement contact stresses for WBT and DTA subjected to various tire inflation pressures (512.0, 690.0, 758.0, and 862.0 kPa) and loads (26.6, 35.5, 44.4, 62.1, and 79.9 kN) were made. The measuring equipment, data processing, and variation of tractions in each direction, along with contact area and maximum contact length, were presented.

Based on the experimental measurements, it was concluded that maximum vertical contact stresses were greater for WBT than for DTA, with the difference increasing as load increased. WBT distributed applied load more uniformly than DTA at low and intermediate loads; at high load, more loads/stresses at the edges of WBT were noted. In addition, tire inflation pressure affected differently and normalized vertical contact stresses. When analyzing the maximum vertical pressure of each loading case, the linear effect of tire inflation pressure on the mentioned maximum was seen if the applied tire loading was low.

Generally speaking, transverse tractions were as high as 40% of vertical pressure for WBT, but those stresses could be as high as 50% for DTA if the load was relatively high. In the case of longitudinal contact stresses, the upper line corresponded to 35% of vertical pressure for DTA and 40% for WBT. Finally, the linear effect of tire inflation pressure on the contact area for both types of tires was observed: greater contact area for DTA (30% higher) and shorter maximum contact length (65% smaller) when compared to WBT.

AKNOWLEDGMENTS

This publication is based on the results from the ongoing pool fund study DTFH61-11-C-00025: The Impact of Wide-Base Tires on Pavement—A National Study. The project is conducted in cooperation with the Illinois Center for Transportation; the U.S. Department of Transportation, Federal Highway Administration; Rubber Manufacturers Associations; and the following DOTs: Illinois, Minnesota, Montana, New York, Oklahoma, Virginia, and Texas.

The contents of this paper reflect the view of the authors, who are responsible for the facts and the accuracy of the data presented herein. The contents do not necessarily reflect the official views or policies of the Illinois Center for Transportation, the Federal Highway Administration, or the participating partners. This paper does not constitute a standard, specification, or regulation. The donation of the tested tires by Michelin is greatly appreciated. Also, the help of Angeli Gamez during the processing of some of the data is recognized.

REFERENCES

Al-Qadi, I. L., Yoo, P. J. (2007). "Effect of surface tangential contact stresses on flexible pavement response." J. Assoc. Asphalt Pav., 76, 663-692.

Anghelache, G., Moisescu, R., Sorohan, S., and Buretea, D. (2011). "Measuring system for investigation of tri-axial stress distribution across the tyre–road contact patch." *Measurement,* 4, 559-568.

Anghelache, G., Negrus, E. M., and Ciubotaru, O. (2003). "Investigation of shear stresses in the tire–road contact patch." SAE Technical Paper 2003-01-127. Society of Automotive Engineers.

Bonse, R. P., and Kuhn, S. H. (1959). "Dynamic forces exerted by moving vehicles on a Road Surface." *Highway Res. Board Bull.,* 233, 9-32.

De Beer, M., Fisher, C., and Jooste, F. J. (1997). "Determination of pneumatic tyre/pavement interface contact stresses under moving loads and some effects on pavements with thin asphalt surfacing layers." *Proc., 8th International Conference on Asphalt Pavements*. Seattle, Washington, USA, 179-227.

Guide for Mechanistic–Empirical Design of New and Rehabilitated Pavement Structures. NCHRP 1-37A Final Report. ARA, Inc., ERES Consultants Division, Champaign, Ill., 2004. http://onlinepubs.trb.org/onlinepubs/archive/mepdg/home.htm

Himeno, K., Kamijima, T., Ikeda, T., and Abe, T. (1997). "Distribution of tire contact pressure of vehicles and its influence on pavement distress." *Proc., 8th International Conference on Asphalt Pavements*. Seattle, Washington, USA, 129-139.

Howell, W. E., Perez, S. E., and Vogler, W. A. (1986). "Aircraft tire footprint forces." *The Tire Pavement Interface, ASTM STP,* 929, 110-124.

Lippmann, S. A., and Oblizajek, K. L. (1974). "The distributions of stress between the tread and the road for freely rolling tires." *Society of Automotive Engineers,* 740072, 1-31.

Myers, L. A., Roque, R., Ruth, B. E., Christos, D. (1999). "Measurement of Contact Stresses for Different Truck Tire Types to Evaluate their Influence on Near-Surface Cracking and Rutting." *Transportation Research Record: Journal of the Transportation Research Board,* 1655(1999), 175-184.

Seitz, N., and Hussmann, A. (1971). *Forces and displacement in contact area of free rolling tires*. New York: Society of Automotive Engineers, 2323-2329.

Tielking, J. T. (1994). "Measurement of truck tire footprint pressures." *Transport. Res. Rec.: J. Transport. Res. Board,* 1435, 92-99.